INTERNATIONAL JOURNAL OF
INNOVATIONS IN SCIENCE & TECHNOLOGY
(ISSN 2618-1630)

IJIST
ISSN : 2618-1630

Volume-2
Issue-2

journal.50sea.com

Prof Dr. Ali Iqtadar Mirza
Chief Editor
International Journal of Innovations in Science and Technology

Abstracting and Indexing

IJIST
P ISSN : 2618-1630
E ISSN : 2909-6130
Recognized Journal

Scientific Journal Impact Factor
TOGETHER WE REACH THE GOAL

Scilit

CiteFactor
Academic Scientific Journals

IOI JOURNALS MASTER LIST

IDEAS

INFOBASE INDEX

IPIndexing
Indexing Portal

RESEARCHBIB
ACADEMIC RESOURCE INDEX

ROOTINDEXING
JOURNAL ABSTRACTING AND INDEXING SERVICE

SIS

WIKIDATA

Instructions for Authors

The editorial board encourages and welcome true researches, laboratory experiments and real time field observations to get published in IJIST. The authors are advised to prepare their manuscript according to the template of IJIST.

Please see the checklist before submitting your manuscript to IJIST.

- The manuscript is prepared according to the template of IJIST.
- Symbols and names are used according to international standards.
- Page no and Line no are adjusted on the manuscript.
- Figure and Table are clearly cited.
- Author names and their affiliation are typed clearly.
- There is no any limit to the length of manuscript.
- Abstract is comprised of 250 words.
- Author's contribution and the statement narrating no of conflict of interest is mentioned in the end.
- Each Figure and Table is numbered and cited in the text.
- Spelling and English grammar is checked.
- It is "Open Access" journal that publish articles on payment of publishing fee by authors or by their institutions.
- All the articles are published under Creative Common License CC-BY therefore, authors mush agree with same license.

Aims and Scopes

The authors are advised to submit their manuscript in accordance with disciplines as below:

- Administrative Science
- Agriculture/Forestry
- Climatology
- Criminology
- Development Study
- Environment
- GIS
- Geography
- Meteorology
- Physics
- Remote Sensing
- Social Science
- Urban Planning
- Economics
- Chemistry
- Bio-Chemistry
- Computer Science

Peer Review Process

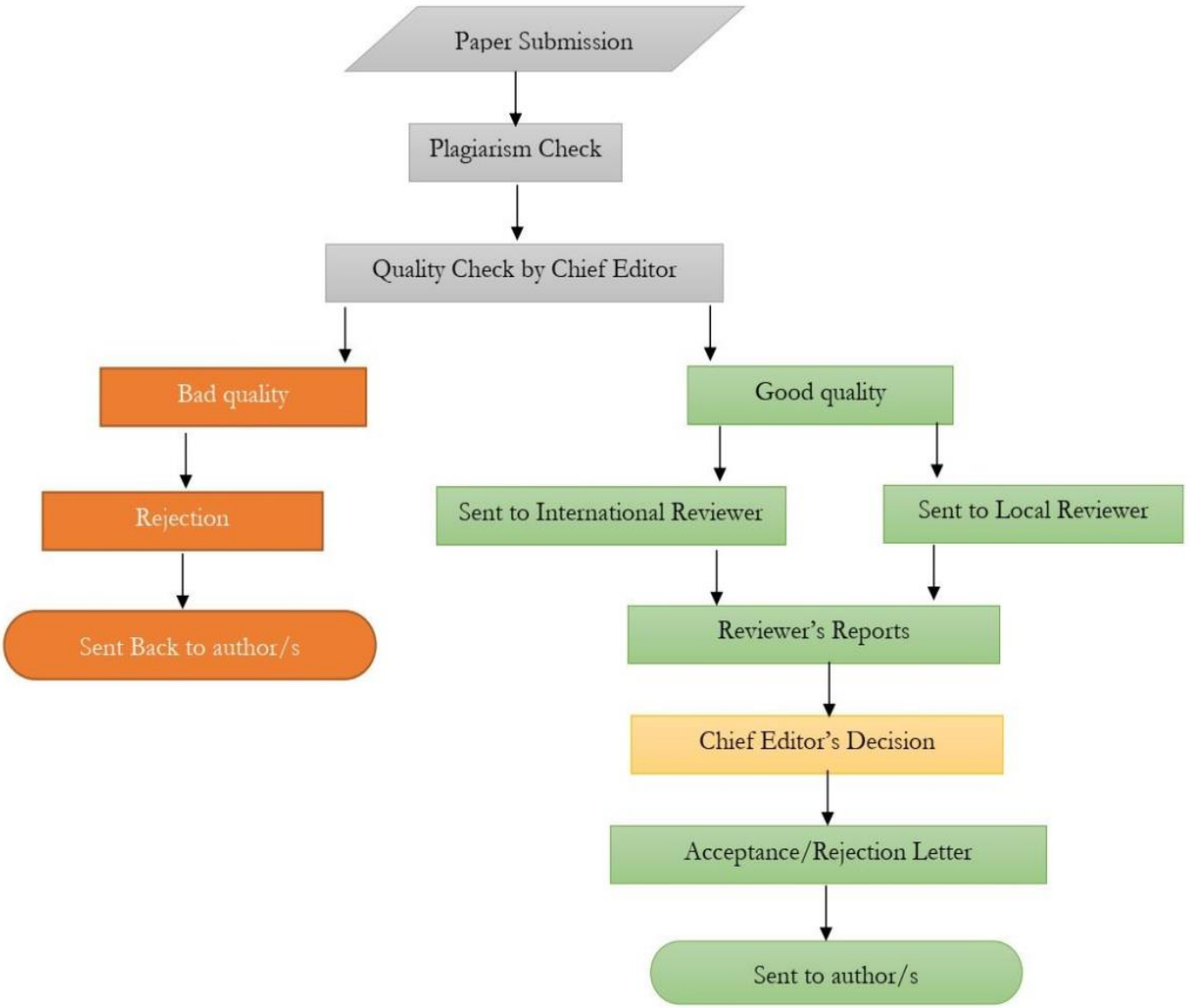

Table of Contents

International Journal of Innovations in Science & Technology (IJIST)

ISSN 2618-1630

V2-I2 | June 2020

50SEA.COM

IJIST
ISSN : 2618-1630

Synthesis of NiO/ZnO Nanoparticles using 2-Propanol Solvent and their Applications for Methylene Blue Degradation

Lubna Noor[1], Bakhtawar Sajjad[2], Auswa Nadeem[2], H. Tanzilla Hussain[3], Shaista Ali[4], Muhamad Akhyar Farrukh[5],

[1] University of Lahore, Pakistan

[2] University of Engineering and Technology, Lahore, Pakistan.

[3] Bahauddin Zakariya University, Multan, Pakistan

[4] Government College University, Lahore, Pakistan

[5] Forman Christian College University, Lahore, Pakistan

*Corresponding Author: Bakhtawar Sajjad bakhtawarsajjad898@yahoo.com

Citation | Noor L, Sajjad B, Nadeem A, Hussain H T, Ali S, and Farrukh M A "Synthesis of NiO/ZnO Nanoparticles using 2-Propanol Solvent and their Applications for Methylene Blue Degradation". International Journal of Innovations in Science and Technology, Vol 02 Issue 02:pp 38-45.

DOI: https://doi.org/10.33411/IJIST/2020020104

Received | January 03, 2020; Revised | February 13, 2020; Accepted | February 25, 2020; Published | March 03, 2020

The nanoparticles play a significant role in fabrication process which are used at large scale in various fields e.g., sensors, electronics drug delivery, optics, catalysis and in water purification process. Nanoparticles (NiO/ZnO) were synthesized using sol-gel technique. In this method, 2-propanol was taken to analyze the particle size. Fourier Transform Infrared Spectroscopy (FT-IR) confirmed the presence of ZnO/NiO. Ultraviolet Visible (UV) data recorded a band gap for ZnO that was 4.1 eV while UV spectrum of methylene blue demonstrated a decrease in concentration of methylene blue while using NiO/ ZnO as catalyst.

Keywords: Sol-gel, Nanocomposites, Methylene blue, Photocatalyst

Introduction:

The existence of nanoparticles in metal oxides are significant while performing fabrication which leads to exchanging their bulk properties. These nanoparticles are widely used in various fields e.g., sensors, electronics drug delivery, optics, catalysis and in water purification process [1]. These nanoparticles have very diverse properties as insulator, metal and semi-conductor which are used in piezoelectric devices, microelectronic circuits and the gas sensors [2]. Zinc oxide are in extraordinary in nature as these have low cost, highly photosensitive and non-toxic. These are usedin solar cells, light emitting diodes, photonic crystals, acoustic wave filters, modulator wave guides, transparent conductors and photo detectors. These nanoparticles are unique due to their properties such as they have a band gap of 3.37ev having energy as 60mev [3-8]. The nanoparticlesof nickel oxide act as cathode in superconductors [9], because these are super paramagnetic and ferromagnetic in behavior [10]. NiO has a band gap 3.5 eV which behave like p-type semiconductors and applied in various fields such as battery manufacturing, electro chromic film, and gas sensors [11-15]. NiO has been investigated extensively due to its structure. The electrons of NiO are spread over a large range of energy due to strong coulomb repulsion [11, 16].

ZnO based nanocomposites are interesting for photocatalytic degradation because various advantages including direct band gap, anisotropic growth, high electron mobility and simple

controlling of its morphology [17]. Montini and co-authors synthesized NiO/ZnO nanocomposite and investigated photocatalytic properties of nanoparticles [18].

The aim of this research is to synthesize NiO/ZnO nanoparticles by using 2 propanol as solvent and the application of these nanoparticles as catalyst for methylene blue dye degradation i.e. a harmful dye.

Material and Methods

$NiCl_2.6H_2O$, Methylene blue and 2-propanol was acquired from sigma Aldrich and $ZnCl_2$ was from Riedl-de-Haen. $ZnCl_2$ was taken 0.013g and $NiCl_2.6H_2O$ was taken 0.024g. Both were dissolved in 10 ml 2-propanol. The pH of this solution was measured as 1. The solution was stirred for 5-minutes at room temperature and raised its pH up to 9. Now this solution was centrifugedat 1300rmp for 2-miniutes. To get dry precipitates, we put these in oven overnight and then calcined for two hours at 450°C to obtain oxides only. The chemical reaction is as below:

$$NiCl_2.6H_2O + ZnCl_2 + 4NaOH \rightarrow 4NaCl + Ni(OH)_2 + Zn(OH)_2 + 6H_2O$$

$$Ni^{2+} + Zn^{2+} + 4OH^- \rightarrow Ni(OH)_2 + Zn(OH)_2$$

Figure 1 is showing the flow of study adopted in this research to get NiO/ZnO nanoparticles.

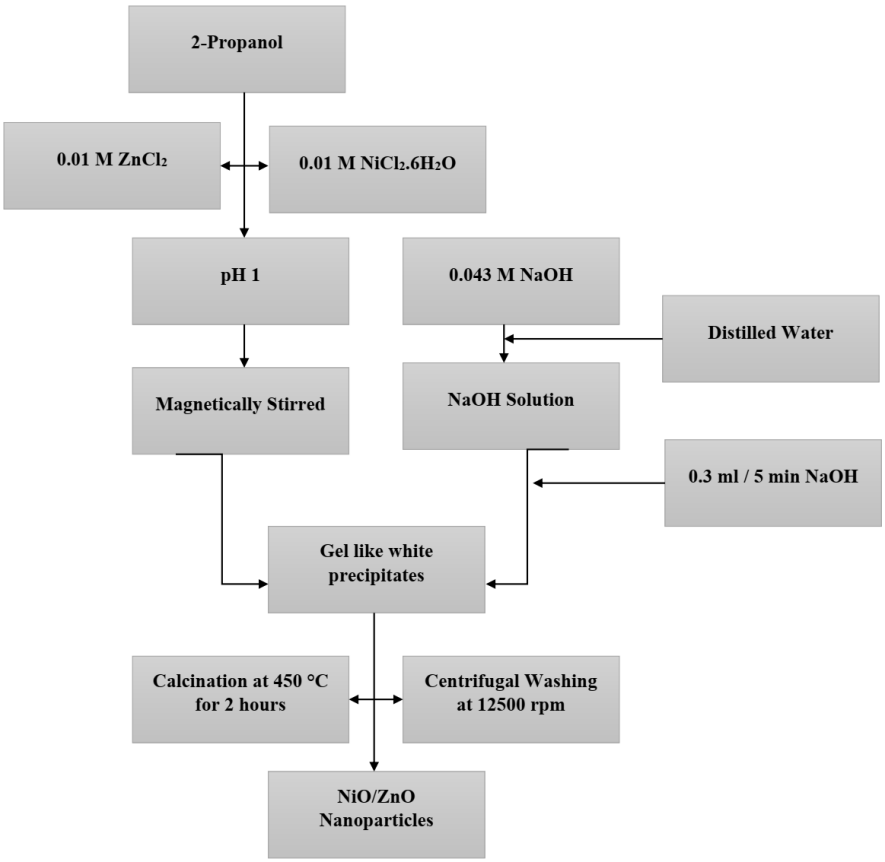

Figure 1 Systematic Synthesis of NiO/ZnO

NiO and ZnO nanoparticles were investigated for photo catalytic activity. A solution of Methylene blue was prepared in 20ppm and passed through ultraviolet spectrometer. The wavelength of this solution was recorded as 659nm. About 20ml of this solution was taken into a separate beaker and 10mg of NiO/ZnO nanoparticles were added in it. This solution was further passed through ultraviolet spectrometer at a wavelength of 659nm and the catalytic activity of NiO/ZnO was measured.

Results and discussion:

Fourier Transmission Infrared Spectroscopy (FT-IR)

FTIR spectrum of NiO/ZnO nanocomposites was recorded after calcination. Figure 2 is showing the percentage of transmittance at various wavenumbers. The broad absorption band was recorded at a wavenumber of about 3350 cm^{-1} which is attributed to O–H stretching vibrations. The band number at 1631 cm^{-1} is attributed to bending mode (H–O–H). The peak at band number 1416 cm^{-1} is due to symmetric stretching of C=O. A peak was recorded around 880.8417 cm^{-1} which was due to metal oxygen bond while the band number at 637.321 cm^{-1} represents the stretching vibrations of Ni-O-H bond. The peak at band number 470.201 cm^{-1} represents the peak of Ni-O nanoparticles. The absorption band at 470.201 cm^{-1} describes the stretching mode of ZnO which lie between 450 cm^{-1} to 500 cm^{-1} The same results were recorded were reported by various researchers [17,18,19,20,21,22,23].

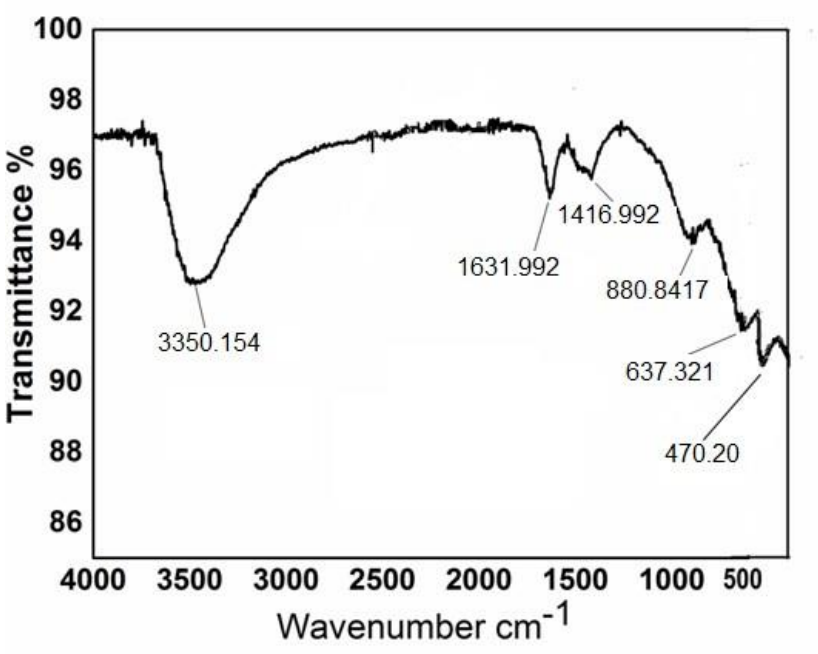

Figure 2 FT-IR of calcined NiO/ZnO

Particle Size Analysis

The particle size of nickel oxide and zinc oxide nanoparticle were measured by taking Bt- 90 analyzer. The results reported that the surface area and the particle size are in inverse relation to each other. Particle size was estimated as 175nm, 139nm, 92nm and 69nm after 1, 2, 3 and 4hours respectively as showing in Table 1 and Figure 3.

Table 1. Relationship between particle size and the surface area of NiO/ZnO using 2-Propanolas solvent.

Time (hours)	Particle Size (nm)	Specific Area m^2/g
1	175	14.24
2	139	18.22
3	92	22.66
4	69	29.69

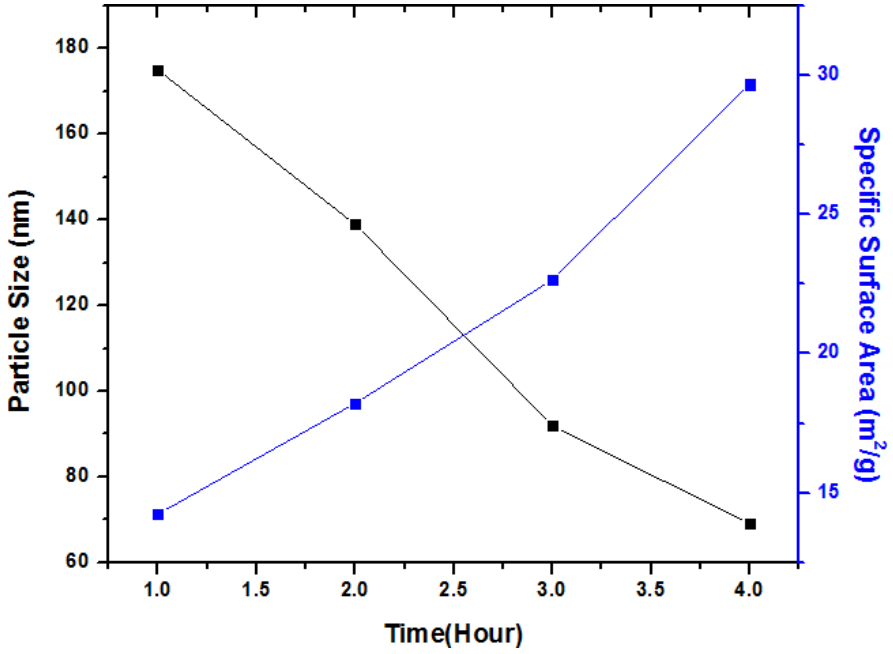

Figure 3 Particle size, time and specific surface area if NiO/ZnO nanoparticles using 2-propanol as solvent

UV- Visible Spectroscopy:

Band gap of NiO and ZnO nanoparticles was measured using the following equation:

$$(h\nu\alpha)^n = A\,(h\nu - E_g) \qquad \text{Eq (1)}$$

In equation (1) "A" indicates the absorption, "Eg" is band gap, "hν" determines the photo energy and "α" represents the absorption coefficient. The value of n is taken as 2 in case of direct transition and ½ for indirect transition.

The band gap of NiO/ZnO was estimated as 4.1ev. Figure 4 is showing the ultraviolet and visible spectrum of NiO/ZnO nanoparticles.

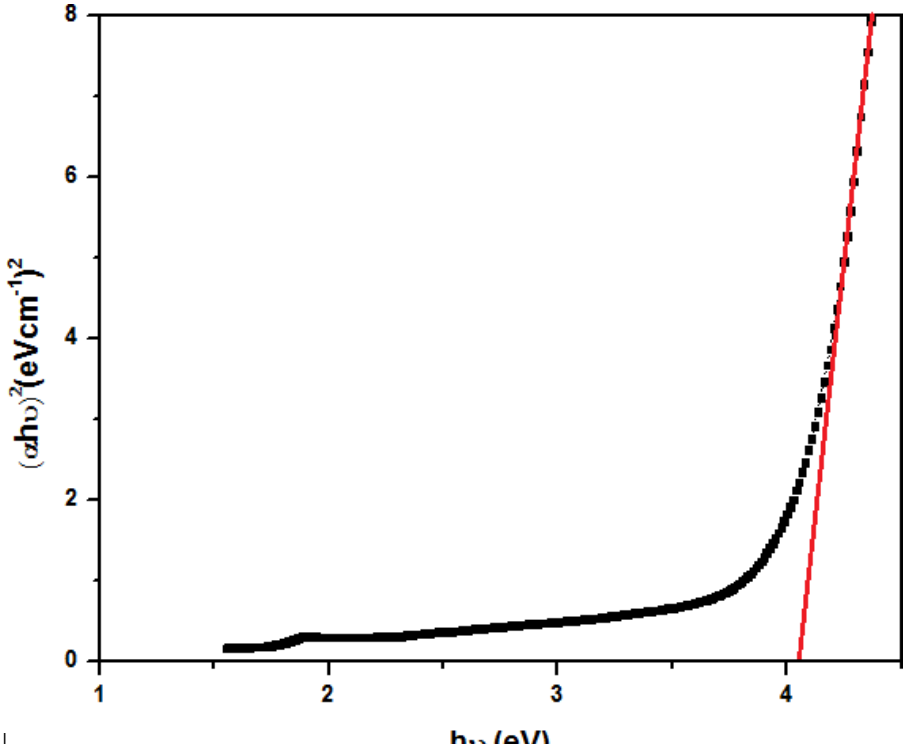

Figure 4: the band gap of NiO/ZnO.

Photocatalytic Activity of NiO/ZnO nanoparticles:

The photocatalytic activity of NiO/ZnO nanoparticles was estimated using UV-visible spectrophotometer with methylene blue. The absorption capacity of the solution was estimated by exposing it to sunlight and the absorption was estimated after every 15 minutes. The absorption capacity was declined with passage of time as shown in Table 2.

Table 2. Photocatalysis data of methylene blue

Sr. No.	Time (min)	Absorbance
1	Blank	2.986
2	0	2.183
3	15	2.313
4	30	2.298
5	45	2.235
6	60	2.138
7	75	1.620
8	90	1.607
9	105	1.573
10	120	1.324
11	135	1.114
12	150	1.022
13	165	0.853
14	180	0.837
15	195	0.672

Figure 5,6 and 7 are clearly representing the catalytic nature of NiO/ZnO nanoparticles worked. Figure 5 is showing the decrease in absorbance with the passage of time confirming the decreasing concentration of methylene blue in the presence of nanoparticles.

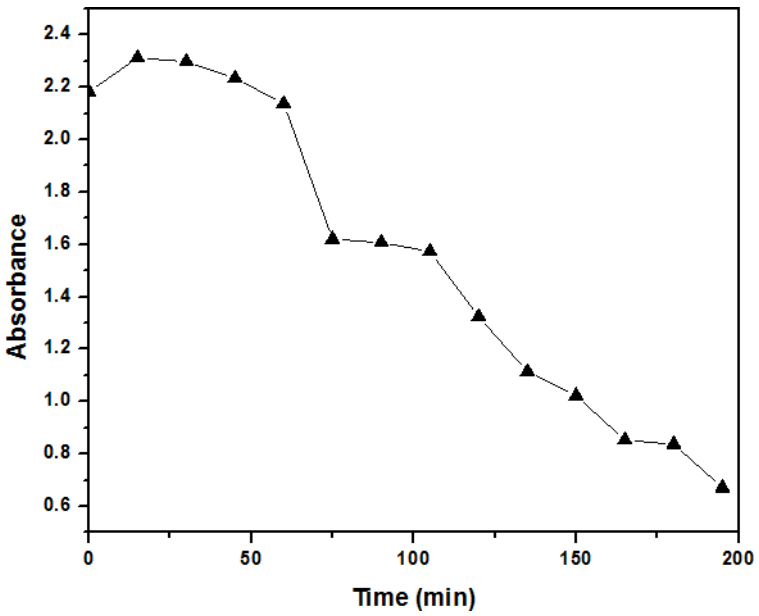

Figure 5 Methylene Blue absorbance with respect to time.Figure 6 is showing that Methylene Blue was degraded with passage of time.

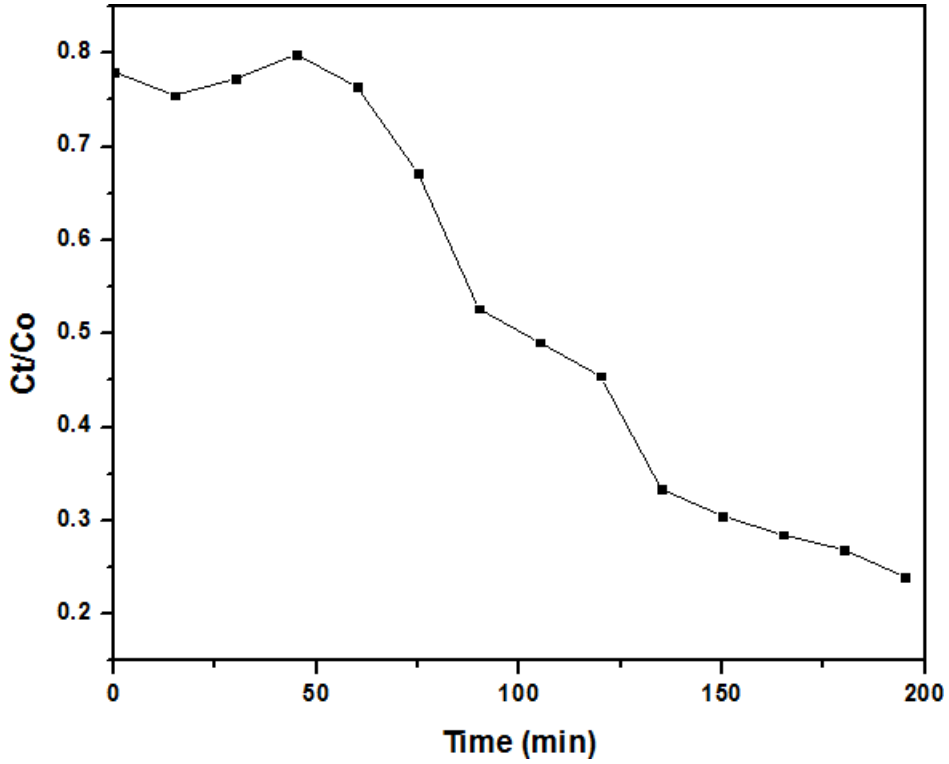

Figure 6 Degradation of MB dye as a function of UV light irradiation time

Figure 7 confirmed that NiO/ZnO nanoparticles degraded the dye up to 75% with passage of time.

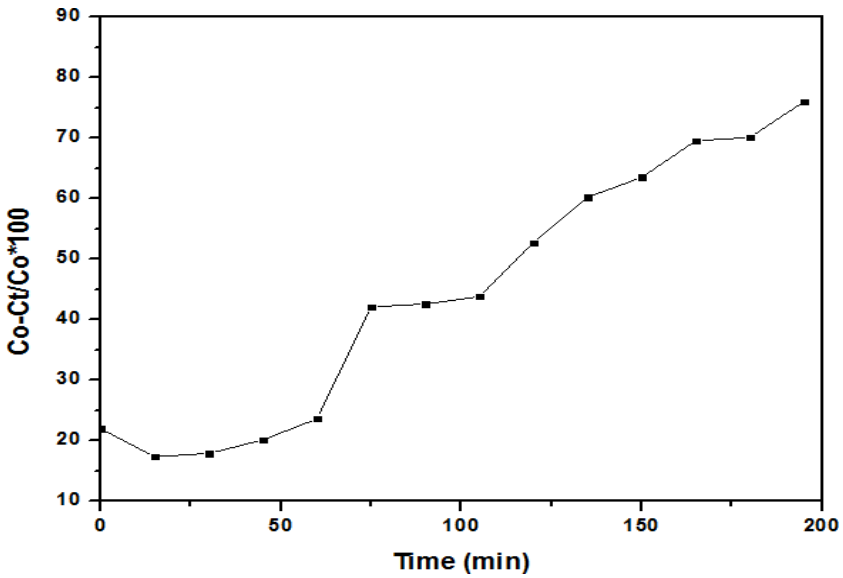

Figure 7 MB degradation efficiency of ZnO NPs

Conclusion:

Nickel oxide and zinc oxide nanoparticles were synthesized using sol-gel method, and the particle size was measured as 69nm and 52.1nm of uncalcined and calcined nanoparticles respectively. A band gap of 4.1ev was measured for NiO and ZnO nanoparticles. Photocatalytic activity of nickel oxide and zinc oxide nanoparticles showed maximum degradation up to 75% under sunlight irradiations. Nickel oxide and zinc oxide nanoparticles can be used as active catalyst for methylene blue degradation.

Acknowledgement. Lubna Noor, Bakhtawar Sajjad, H.Tanzilla Hussain and Auswa Nadeem are sincerely thankful to Government College University, Muhammad Akhyar Farrukh and Shaista Alifor conducting this research.

Author's Contribution. All the authors contributed equally.

Conflict of interest. We declare no conflict of interest for publishing this manuscript in IJIST.

Project details. NIL

References:

1. Maynard, Andrew & Aitken, Robert & Butz, Tilman & Colvin, Vicki & Donaldson, Ken& Oberdörster, Günter & Philbert, Martin & Ryan, John & Seaton, Anthony & Stone, Vicki & Tinkle, Sally & Tran, Lang & Walker, Nigel & Warheit, David. Safe handling of nanotechnology. Nature. 444: 267-9 (2006).
2. Zhang, F., Chan, S.W., Spanier, J., Apak, E., Jin, Q., Robinson, R., Herman, I. Cerium oxide nanoparticles: size-selective formation and structure analysis. Appl. Phys. Lett. 80(1):127-129 (2002).
3. Piva, D.H., Piva, R.H., Rocha, M.C., Dias, J.A., Montedo O.R.K., Malavazi, I., Morelli, M.R. Antibacterial and photocatalytic activity of ZnO nanoparticles from $Zn(OH)_2$ dehydrated by azeotropic distillation, freeze drying, and ethanol washing. Advanced Powder Technology 28:463 (2017).
4. Sood, S., Kumar, A., Sharma, N. Photocatalytic and Antibacterial Activity Studies of ZnO Nanoparticles Synthesized by Thermal Decomposition of Mechanochemically Processed Oxalate Precursor. Chemistry select. 1: 2016, 6925.
5. Kavitha, T., Iyengar, A., Gopalan, llLee, K.P., Park, S.Y. Glucose sensing, photocatalytic and antibacterial properties of graphene–ZnO nanoparticle hybrids Carbon. 50: 2994 (2012).
6. Elavarasan, N., Kokila, K., Inbasekar, G., Sujatha, V. Evaluation of photocatalytic activity, antibacterial and cytotoxic effects of green synthesized ZnO nanoparticles by Sechium edule leaf extract. Research on Chemical Intermediates. 43: 3361 (2017).
7. Pradeev Raj, K., Sadaiyandi, K., Kennedy, A., Sagadevan, S. Photocatalytic and antibacterial studies of indium-doped ZnO nanoparticles synthesized by co-precipitation technique. Journal of Materials Science: Materials in Electronics. 28: 19025 (2017).
8. Reddy Yadav, L.S., kumar, D., Kavitha, C., Rajanaika, H., Daruka Prasad, B. Antibacterialand Photocatalytic activities of ZnO Nanoparticles : Synthesized using Water Milon Juice as Fuel. International Journal on Nanoscience. 15: 1 (2016).
9. Wang, D.W., Li, F., Cheng, H.M. Hierarchical porous nickel oxide and carbon as electrode materials for asymmetric supercapacitor. Journal of Power Sources 185(2): 1563-1568 (2008).
10. Ichiyanagi, Y., Wakabayashi, N., Yamazaki, J., Yamada, S., Kimishima, Y., Komatsu, E., Tajima, H. Magnetic properties of NiO nanoparticles. Physica B:Condensed Matter 329: 862-863 (2003).
11. Park, Y.R., Kim, K.J. Sol-gel preparation and optical characterization of NiO and $Ni1-_xZn_xO$ *thin films.* Journal of Crystal Growth 258: 380-384 (2003).
12. Curri, M.L., Agostiano, A., Mavelli, F., Della Monica, M. Reverse micellar systems: self organised assembly as effective route for the synthesis of colloidal semiconductor nanocrystals. Materials Science and Engineering 22: 423-426 (2002).
13. Yoshio, M., Todorov, Y., Yamato, K., Noguchi, H., Itoh, J.I., Okada, M. Mouri, T. Preparation of $LiyMn_xNi1-_xO_2$ as cathode for lithium-ion batteries. Journal of Power Sources 74(1): 46-53 (1998).
14. Yang, H.X., Dong, Q.F., Hu, X.H., Ai, X.P., Li, S.X. Preparation and characterization of $LiNiO_2$ synthesized from $Ni(OH)_2$ and $LiOH.H_2O$. Journal of Power Sources 79(2): 256-261(1999).

15. Miller, E.L., Rocheleau, R.E. Electrochemical Behavior of Reactivity Sputtered Iron-Doped Nickel Oxide . Journal of Electrochemical Society 144(9): 3072-3077 (1997).

16. Bengone, O., Alouani, M., Ch,l P., Hugel, J. Implementation of the projector augmented-wave LDA+U method: Application to the electronic structure of NiO. Phys. Rev. B: Condens. Matter Mater. Phys., 62: (2000).

17. Kovalenko, A.A., Baranov, A.N., Panin, G.N. Synthesis of ZnO/NiO nanocomposites from ethanol solutions. Russ. J. Inorg. Chem., 53(10): 1546–1551 (2008)

18. Hameed, A., Montini, T., Gombac, V., Fornasiero, P. Photocatalytic decolourization of dyes on NiO-ZnO nano-composites. Photochem. Photobiol.Sci., 8(5): 677-682 (2009).

19. Zak, A.K., W.H, Abd M., Darroudi, M., Yousefi, R. Synthesis and characterization of ZnO nanoparticles prepared in gelatin media. Mater.Lett. 65: 70-73 (2011).

20. Meybodi, S., Mohseni, Hosseini, S.A., Rezaee, M., Sadrnezhaad, S.K., Mohammadyani, D. Synthesis of wide band gap nanocrystalline NiO powder via a sonochemical method. Ultrasonics sonochemistry, 19(4): 841-845 (2012).

21. Saad, F., Oboudi, Nadir, F., Habubi, Ghuson, H., Mohamed, Sami, S.,Chiad. Composition and Optiocal Disprsion Characterization of Nanoparticles ZnO NiO Thin Films: Effect of Annealing Temperature. International Letters of Chemistry, Physics and Astronomy, 8(1): 78-86 (2012).

22. Alagiri, M., Ponnusamy, S., Muthamizhchelvan, C. Synthesis and characterization of NiO nanoparticles by sol–gel method. Journal of Materials Science: Materials in Electronics, 23(3): 728-732 (2012).

23. Dutta, S., Ganguly, B.N. Characterization of ZnO nanoparticles grown in presence of Folic acid template. J Nanobiotechnol. 10: 29 (2012).

50SEA.COM

IJIST
ISSN : 2618-1630

COVID-19 Pandemic: A Remedial Measure Through Convalescent Serum

Shahzada Nadeem Abbas[1], Umber Rauf[2], Afshan Saleem[3], Natasha Saleem[4], Tayyba Basheer[5], Sidra Yaseen[4], Nida Irfan[4] and Asif Naushad[6].

[1] Department of Biology
[2] Veterinary research institute
[3] Department of chemistry/UET Lahore
[4] Department Zoology LCWU
[5] Government College University Lahore
[6] Department of Physical Health Education, PU Lahore.

* Correspondence: Shahzada Nadeem AbbasE-mail: shazadanadeemabbas@lu.edu.pk

Citation |Abbas.N.A., Rauf. U., Saleem. A., Saleem. N., Basheer.T.,Yaseen.S., Irfan.N., Naushad. A "COVID-19 Pandemic: A Remedial Measure Through Convalescent Serum". International Journal of Innovations in Science & Technology, Vol 02 Issue 02: pp 46-50, 2020.

Received | April 15, 2020; Revised |May 05, 2020; Accepted | June 18, 2020; Published | June 21, 2020.

An acute respiratory syndrome Corona Virus 2 has affected humanity throughout the world. Scientifically, Corona Virus 2 is known as SARS-COV-2 which is abbreviated as COVID-2019. China was the first victim of this outbreaks in December 2019 [1] which was later recognized as pandemic on March 11, 2020 by World Health Organization (WHO) [2,3]. At the time of this writing, about 8.75 million individuals of 188 countries [4] have been effected by COVID resulting in 463000 deaths primarily, corona virus communicates from one body to another body through close contacts via droplets produced by sneezing, coughing or taking by infected badly within a buffer zone of 3 to 6 feet [5,6,7]. These droplets fall onto a surface and can survive up to 72 hours [8]. Various studies have proved that droplets may travel up to 37 feet by an uncovered cough [9,10,11]. Corona virus is not an airborne, however it may transport through respiratory droplets during talking and breathing [12].

It may be spread due to contaminated surface by corona including skin touches to eyes, nose, or mouth. Corona virus reacts differently for different surfaces like a stainless-steel surface and plastic surface make corona virus alive up to 3 days, cupboard for one day and copper for four hours [13]. The survival of corona virus is largely dependent upon humidity and temperature [14] where cold temperatures are considered as favorable for corona virus to survive for long times. Currently there is no vaccine or drug to fight against COVID-19 virus, however rapid developments are on the way and may be available in short

times. The most appropriate option of treatment of COVID-19 disease is human convalescent serum.

About 4.33 million individuals have been recovered from COVID-19 disease who can donate serum containing immunoglobin. Antibody therapy is related to immunotherapy which is applied with actively and passively. A specific amount of drug is applied to infected body agent specific anti-agents to activate immune system to produce long term antibodies while passive antibody therapy is concerned with consistent antibody concentration, therefore, passive antibody therapy provides immediate immunity to an infected person.

Viral neutralization is the most adopted mechanism in passive antibody therapy to cure COVID-19, however phagocytosis and cytologist-based mechanisms are also available convalescent sera obtained from COVID-19 recovered patients is the most appropriate deposit antibodies used for treatment of SARS cov-2. Various efforts are on the way to prepare antibodies again COVID-19 but only antibody which can be used immediately is the human convalescent sera. Antibodies work to neutralize inoculum and to modify the inflammatory response which may be achieved with human immune responses [15]. It is observed that passive antibody therapy is effective to apply immediately as soon as the symptoms appear but it becomes less effective as the time passes like on third or fourth day [16]. An appropriate amount of therapy is applied to suspected person which will circulate in tissues and blood to provide agitation against certain infections.

Convalescent has been widely used for curing viral diseases including measles [17,18] influenza [19], and poliomyelitis [20] and mumps [21]. Convalescent sera behaved differently for a variety of viral diseases and results proved different efficiency for each disease. H1N1 2009 virus was treated through convalescent serum antibody during 2009-2010 [22]. Ebola epidemic was also treated through convalescent serum antibody during 2013. The treatment of H3N1 [23] and avian flu H7N9 [24] outbreaks were also cured by serum transformation which kept alive all patients.

Middle East respiratory syndrome and SARS 1 were two epidemics of twenty first century which resulted in high mortality. There was not any effective therapy for curing both epidemics but convalescent serum was used for their treatments [25]. SARS attacked three patients in Taiwan and all were survived by injecting 500ml of convalescent serum. Similarly, three patients struck by MERS in South Korea were cured by applying convalescent serum which resulted in neutralizing antibody [26]. The titer responses are not same in everybody recovered from viral disease but vary from person to person. An analysis was performed in this regard by collecting 99 samples from recovered persons and found that12 of them had absence of antibody [27]. It suggests that everybody does not have equal number of antibodies, it is also observed that the concentration of antibodies changes with time, as some has high and some has low titer response [22-27]. Convalescent serum has been excessively used in China for treatment of COVID-19 which reduced virus up to the extent that life started running normally after a long-term lockdown.

COVID-19 sera are useable for both treatment of diseases or infections. In prophylactic mode, serum prevent infection to whom who are highly vulnerable to disease such kind of treatment was already used to cure various kind of diseases e.g. rabies and

hepatitis B which were treated with hepatitis rabies immune globulin (HR1G) and hepatitis B immune globulin (HB1G) respectively. Mostly infants are hit by severe Respiratory Syncytial Uirus (RSU) which is also treated by passive antibody administration.

Passive administration is also relay and its risks are categorized in two ways; known and theoretical. The known risks are linked to transportation of blood substance which is associated to infection due to another disease agent, and the reaction of serum constituents such as serum sickness. Such kind of risks has become lower by adopting modern techniques of blood banking that screen out blood-borne pathogens. The theoretical risk includes the Antibody Dependent Enhancement (ADE) infection that involve the enhancement of disease due to existence of certain antibodies. A variety of mechanisms for ADE have been adopted and the results show that one type of corona virus may enhance the infection to viral stain [28]. A major theoretical risk is exposure of antibodies before SARS-COV-2 which prevents disease in such a way that infects the human's immune system and produce such individuals that cause reinfection. Both known and theoretical risks can be avoided once a vaccine is available.

Finally, the anecdotal and historical applications of convalescent serum recommends that it is safe to cure COVID-19, particularly aged persons, however a risk-benefit assessment must be executed before the application of convalescent serum.

Deployment of convalescent serum:

The deployment of convalescent serum is conducted in the sequential steps:

(1) Availability of donors who have recovered from this disease and are ready to donate serum.
(2) Modern blood banking facility to pressure serum.
(3) Availability of serological arrays to identify SARS-COV-2 and the biological arrays to compute viral neutralization.
(4) Laboratory to execute the assays.
(5) Chemical trials to examine immune responses.
(6) Regulatory compliance institutional approval depending upon location. Various pharmaceutical companies are trying to generate purified high titer of neutralizing antibodies against COVID-19 but it would be available after many months and the available human sera is the most immediate solution of COVID-19.

The antibody isolation and the serum preparation may be conducted through apheresis from the blood of the COVID-19 recovered in individual if regulatory permissions are on the way. Today nurses, physicians and the health care providers have to face known COVID-19 cases and are also infected. They are sent to quarantine. If such individuals are treated with convalescent serum, quarantine period may be avoided, and it would be helpful to perform their duties. Finally, convalescent serum is the only option that can be used as the most secure and immediate action before preparation of COVID-19 vaccine.

References:

[1]. https://www.who.int/csr/don/12-january-2020-novel-coronavirus-china/en/ (Accessed on 9 April 2020).

[2]. "Statement on the second meeting of the International Health Regulations (2005) Emergency Committee regarding the outbreak of novel coronavirus (2019-nCoV)". World Health Organization. 30 January 2020

[3]. "WHO Director-General's opening remarks at the media briefing on COVID-19—11 March 2020". World Health Organization Retrieved 11 March 2020.

[4]. "COVID-19 Dashboard by the Center for Systems Science and Engineering (CSSE) at Johns Hopkins University (JHU)". ArcGIS. Johns Hopkins University. Retrieved 6 May 2020.

[5]. "Coronavirus Disease 2019 (COVID-19)—Symptoms". Centers for Disease Control and Prevention. 20 March 2020. Retrieved 21 March 2020.

[6]. "Interim Clinical Guidance for Management of Patients with Confirmed Coronavirus Disease (COVID-19)". Centers for Disease Control and Prevention. 4 April 2020. Retrieved 11 April 2020.

[7]. Velavan TP, Meyer CG (March 2020). "The COVID-19 epidemic". Tropical Medicine & International Health. 25 (3): 278–280. doi:10.1111/tmi.13383.

[8]. "Here Comes the Coronavirus Pandemic: Now, after many fire drills, the world may be facing a real fire". Editorial. The New York Times. 29 February 2020. Retrieved 1 March 2020.

[9]. "Symptoms of Novel Coronavirus (2019-nCoV)". US Centers for Disease Control and Prevention. 10 February 2020. Retrieved 11 February 2020.

[10]. Spinney L (29 March 2020). "Coronavirus vaccine: when will it be ready?". The Guardian. ISSN 0261-3077. Retrieved 29 March 2020.

[11]. "Coronavirus public information campaign launched across the UK". Government of the United Kingdom. Retrieved 8 February 2020.

[12]. Kampf G, Todt D, Pfaender S, Steinmann E (March 2020). "Persistence of coronaviruses on inanimate surfaces and their inactivation with biocidal agents". The Journal of Hospital Infection. 104 (3): 246–251. doi:10.1016/j.jhin.2020.01.022

[13]. Coronavirus disease 2019 (COVID-19) Situation Report—73". World Health Organization. 2 April 2020. Retrieved 3 April 2020.

[14]. Coronavirus disease (COVID-19) advice for the public: When and how to use masks". World Health Organization. Archived from the original on 7 March 2020. Retrieved 9 March 2020.

[15]. Kuo, Lily (21 January 2020). "China confirms human-to-human transmission of coronavirus". The Guardian. Retrieved 18 April 2020.

[16]. Casadevall A, Scharff MD. Serum therapy revisted: animal models of infection and development of passive antibody therapy. Antimicrob Agents Chemother. 1994;38(8):1695–1702.

[17]. Park WH. Therapeutic use of antipoliomyelitits serum in preparalytic cases of poliomyelitis. JAMA. 1932;99:1050–1053.

[18]. Park WH, Freeman RG. The prophylactic use of measles convalescent serum. JAMA. 1926;87(8):556–558.

[19]. Gallagher JR. Use of convalescent measles serum to control measles in a preparatory school. Am J Public Health Nations Health. 1935;25(5):595–598.

[20]. Rambar AC. Mumps; use of convalescent serum in the treatment and prophylaxis of orchitis. Am J Dis Child. 1946;71:1–13.

[21]. Luke TC, Casadevall A, Watowich SJ, Hoffman SL, Beigel JH, Burgess TH. Hark back: passive immunotherapy for influenza and other serious infections. Crit Care Med. 2010;38(4 suppl):e66–e73.

[22]. Hung IF, et al. Convalescent plasma treatment reduced mortality in patients with severe pandemic influenza A (H1N1) 2009 virus infection. Clin Infect Dis. 2011;52(4):447–456.

[23]. Kong LK, Zhou BP. Successful treatment of avian influenza with convalescent plasma. Hong Kong Med J. 2006;12(6):489.

[24]. Zhou B, Zhong N, Guan Y. Treatment with convalescent plasma for influenza A (H5N1) infection. N Engl J Med. 2007;357(14):1450–1451.

[25]. Wu XX, Gao HN, Wu HB, Peng XM, Ou HL, Li LJ. Successful treatment of avian-origin influenza A (H7N9) infection using convalescent plasma. Int J Infect Dis. 2015;41:3–5.

[26]. Cheng Y, et al. Use of convalescent plasma therapy in SARS patients in Hong Kong. Eur J Clin Microbiol Infect Dis. 2005;24(1):44–46.

[27]. Ko JH, et al. Challenges of convalescent plasma infusion therapy in Middle East respiratory coronavirus infection: a single centre experience. AntivirTher (Lond). 2018;23(7):617–622.

[28]. Gajic O, et al. Transfusion-related acute lung injury in the critically ill: prospective nested case-control study. Am J Respir Crit Care Med. 2007;176(9):886–891.

50SEA.COM

IJIST
ISSN : 2618-1630

Active Surface deformation from DEM Based Surface Dynamics in Upstream of Mangla Reservoir and eastern Potwar Plateau

Rao Mansoor Ali Khan[1], Azam Sohail[1], Syeda Areeba Gillani[1], Syed Shehzad Hassan[1], Syed Amer Mahmood[1]

[1] Department of Space Science University of the Punjab Lahore.

* Correspondence: Rao Mansoor Ali Khan: raomansor@gmail.com

Citation | Khan.R.M.A, Sohail.A, Gillani.S.A, Hassan.S.S, Mahmood.S.A "Active Surface deformation from DEM Based Surface Dynamics in Upstream of Mangla Reservoir and eastern Potwar Plateau" International Journal of Innovations in Science and Technology Vol 02 Issue 02: pp 51-60, 2020.

Received |May, 15 2020; Revised | June 01, 2020; Accepted | June 12, 2020; Published | June 14, 2020.

Digital Elevation Model (DEM) acquired by Shutter Radar Topographic Mission (SRTM) is useful to compute Surface Dynamics (SDs) including, Drainage Density (DD), Topographic Relative Relief (TRR), Iso Base-Levels (IBL) and Topographic Vertical Dissection (TVD). It provides detailed information about the lithology based on erosional boundaries as well as delineation of active tectonic scarps. It confers a well-built connection among diverse stream Strahler ordering and the localized erosive or neotectonics conditions in an actively deforming topography. These techniques are rapid, proficient, and consistent to demarcate tectonic control even along or over the similar lithologies. This investigation appraises the eroding and uplifting landforms along upstream of Mangla reservoir in lower Jhelum valley. The aim is to delineate margins for lithological demarcation and to distinguish whether these are affected by neotectonics or not. We noticed unusual local-base-level inconsistency that may be related to the well-known active tectonic expressions.

Keywords: SRTM DEM, Surface dynamics, local base level, drainage density, topographic relative relief, topographic vertical dissection and Mangla reservoir.

1. Introduction.

The continental plates are pulverized with each other by head to head which are subducted and superseded e.g. Indian plate has been subducted by Eurasian plate therefore, it is broken from various points which are called the fault zones [1]. A pressure is induced underneath these plates due to which the rocks are twisted, pressed, or elongated. The strain underneath these rock units enhances and a point comes beyond which these plates get burst and spread [2]. This discharge of energy is impulsive in nature which trigger the seismic waves to move in all directions from the epicenter [3]. The result of these scenarios is lethal which cause massive earthquakes, landslides, continental rifting, active faulting, and devastating tsunamis [4]. The Topographic Relative Relief (TRR) has become a significant issue for man-

oriented environment. The TRR and cartograph are in inverse relation to physical science relating to earth's surface.

The utilization of Digital Elevation Model (DEM) in various fields of life has motivated researchers to visualize mountainous topography in 3D to determine attitudinal variations [5]. GIS based datasets along with earth surveillance data is widely used in investigation of geomorphometric indices [6]. These investigations have resulted in modeling of terrain geologically and hydrologically.

Morphometry is a term used for investigation of topography based on arithmetic measurements of landforms [7]. These indices are capable of investigating the TRR characteristics of a region [8]. Lower Jhelum valley is comprised of topography with changing elevations, dimensions, magnitudes, and scales. The estimation of topography relief requires the detailed information of slope and aspect.

The main objective of this research was to investigate study site using seven surface indices including Topography Slope (TS), Drainage Density (DD), Topography Aspect (TA), Topography Vertical Direction (TVD), Iso Base Level (IBL), Hack Gradient index (HGI) and Topographic Relative Relief (TRR). The Satellite Remote Sensing (SRS) and GIS built-in procedures are capable to evaluate the above mentioned seven indices using DEM. Therefore, the basic input was the acquisition of high resolution, dipressionless DEM which is geometrically accurate.

Study Site:

Potwar plateau is situated at a latitude 33-34N and at 73-74E longitude, having surprising topography. The study site has its topographic importance due to Main Boundary Thrust (MBT) in the NW and NE direction [9]. Some unique structures e.g., Risai and Kotli thrust is located in SE-NW direction and the Jehlum fault is oriented in the same fashion. Rawat thrust is in SE-NE direction which expresses various surface deformation styles existing over or beneath the surface [10]. The test site is a deformed part of western Himalayan fold mentioned in Figure 1, having Neogene deformations surged in south to salt range thrust, in comparison to MBT. The lineaments and outcrop trends are roughly at right angle to the movements of tectonic structures, having average shortening of 16mm/year [11]. Figure 1 (b) is showing the location of study area with earthquakes locations in red and thick 273 black lines represent thrust faulting with teeth symbols showing direction 274 of thrust movements.

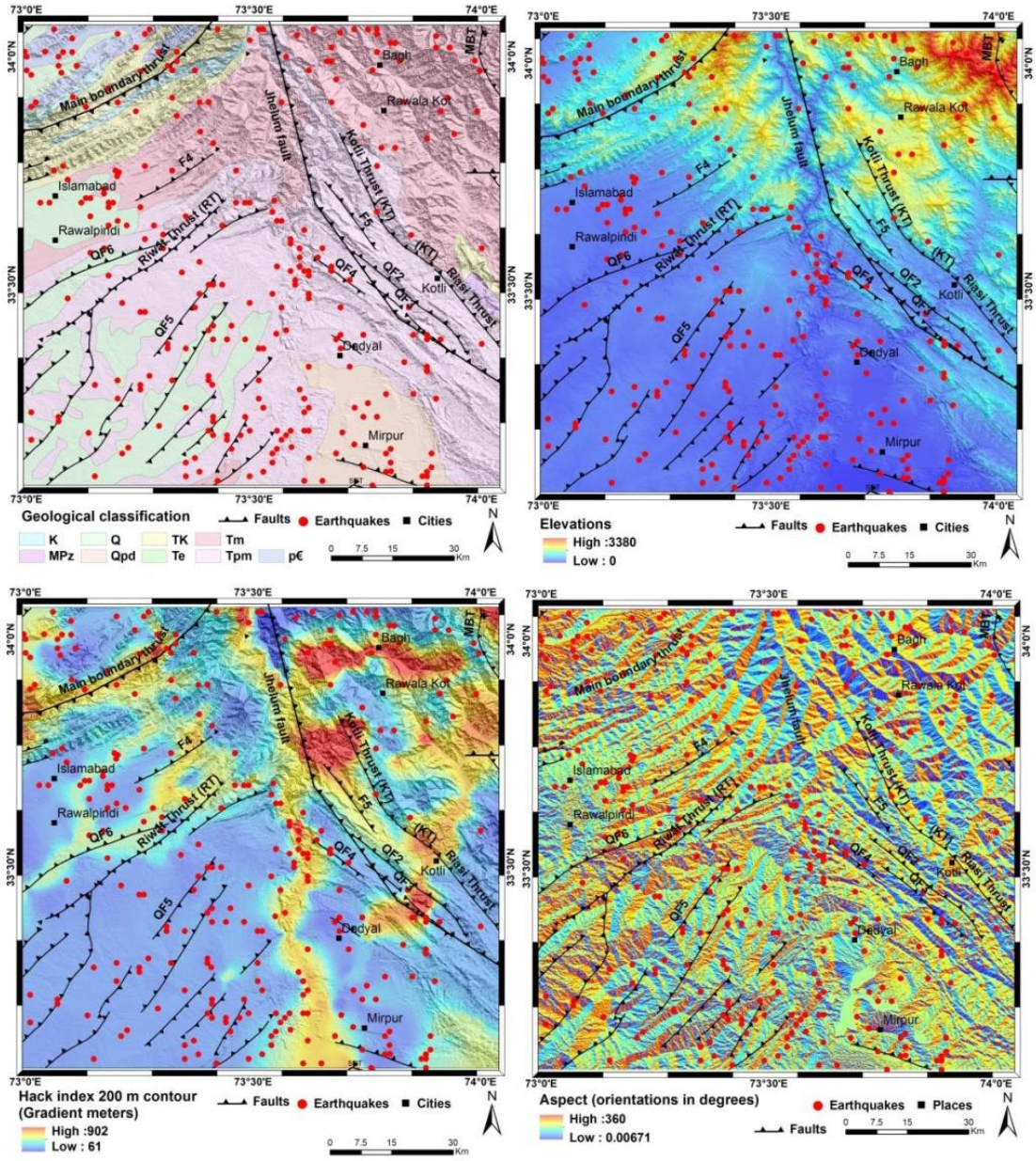

Figure 1. (a) Geology Map, (b) Investigation Site, (c) Hack Gradient message and (d) Aspect map.

Materials and Methods:

SRTM DEM is freely available for downloading from Global Land Cover Facility (GLCF) in Tagged Information File Format (TIFF) with 30m resolution. The study site was analyzed for various indices including HGI, TA, TS, TVD, IBL, DD and TRR and examined the geometric grids for each procedure. The slope gradient algorithm (SGA) expresses high correlations for formulation of dissimilar results. The SGA along with aspect map provides raw values to be used in eigenvector algorithm, therefore the SGA may affect the final output. [10] introduced Steepest Adjacent Neighborhood Algorithm (SANA), however the four

nearest neighborhood algorithm (FNNA) is most authentic and widely used algorithm according to [11]. The eight-neighborhood algorithm was introduced by EVANS [12]. A dissimilarity between FNNA and SANA explore the impacts of SANA on geomorphometric factors. Slope of topography was computed using eight-neighborhood algorithm. SANA was employed to compute singular solitary and slope values at the mid location [13]. The illustration of Iso base and TVD mechanism is shown in Figure 2,

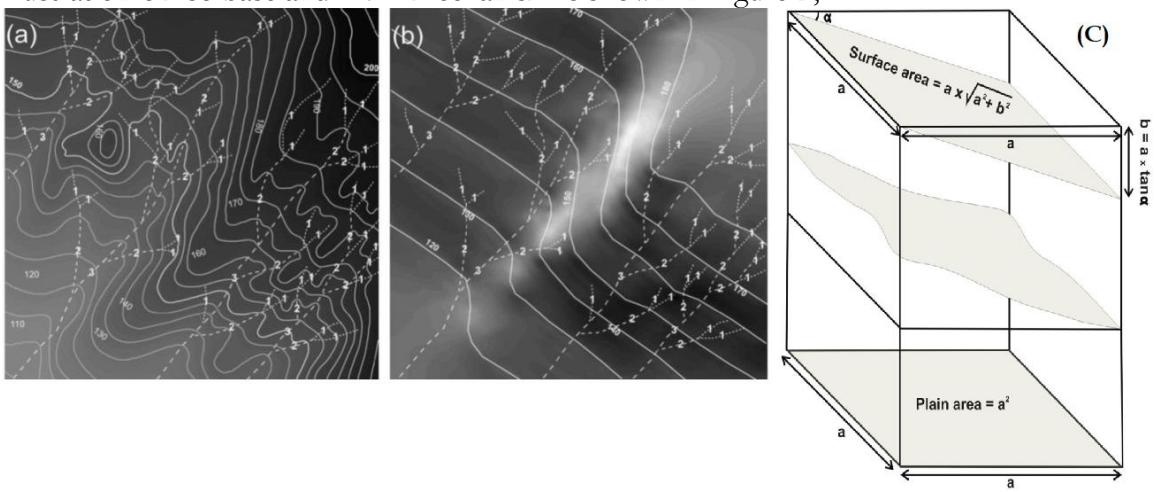

Figure 2. (a,b) Illustration of Iso base and (c) TVD mechanism.

Results and discussion:

The geomorphometric indices which were analyzed includes Iso base level (IBL), Drainage Density (DD), Topography Vertical Direction (TVD), and Topographic Relative Relief (TRR). These indices are capable to isolate landforms into a number of morphometric units to evaluate the hydrologic environments and subcategories of landforms. The geographic and spatial distribution of study site is explained below.

The IBL were obtained from 2nd or 3rd Strahler order coding and the results are mapped in Figure 3.

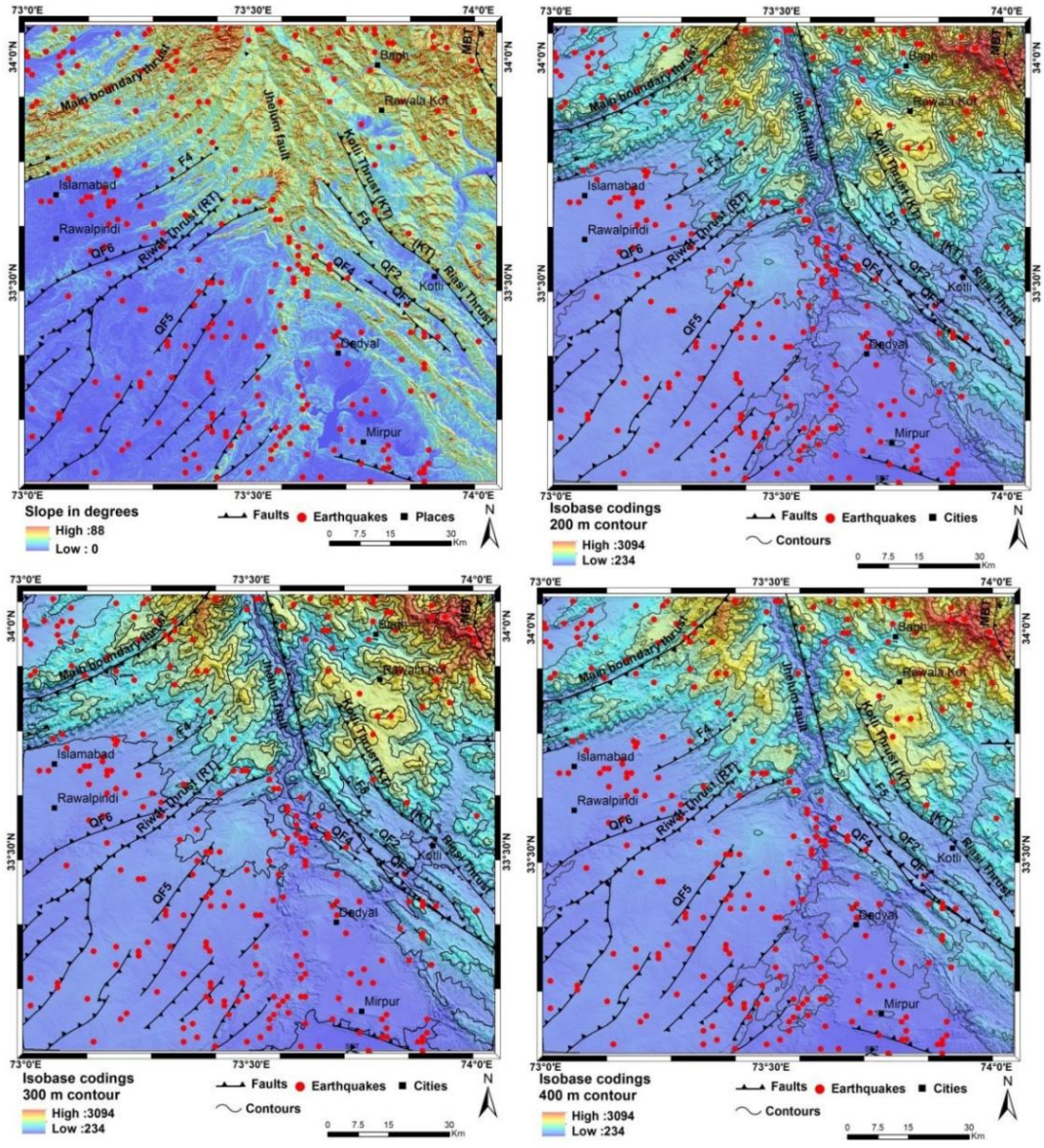

Figure 3. (a) Slope map showing slope variation in degree while red showing steep slopes and cyan region with less gentle slopes, (d) Slope map showing various Isobase maps with isobase contour lines with a spatial interval of 200 m, 300 m and 400 m.

The lineaments were extracted using SRTM DEM. The NNW-SE and NE-SW directed fault lines are directly linked with configuration of study area as shown in Figure 1. The Eastward orientation of Iso-base level lines directed in NE-NNW direction over inflexion of Nelum and Jehlum rivers. It was identified that the SW and NE orientation of IBL lines transvers to NW-SE of iso-base lines and Kotli and Riasi faults were identified.

Drainage density (DD)

Drainage density (DD) was computed by taking stream length per channel per hundred square kilometer area. DD can be influenced by various factors e.g., climate,

geology/lithology and soil types [9]. DD is further subdivided in five different classes as below in Figure 4

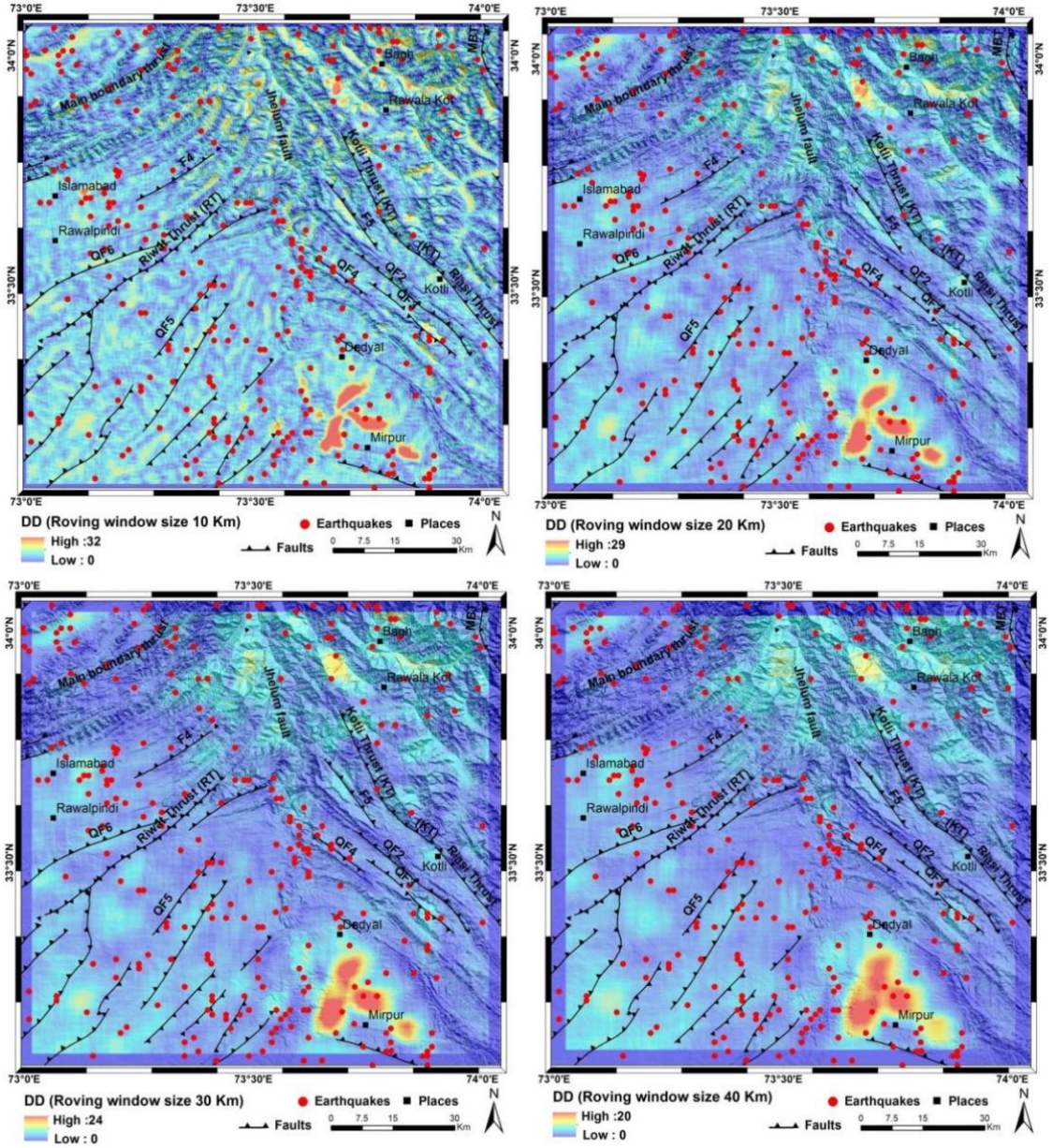

Figure 4. Drainage density maps extracted from SRTM DEM with variable spatial roving window sizes of 10, 20, 30 and 40 m

Almost 50% of study area was found under intermediate DD, which may be due to presences of majority of hard rocks and less uplift rates with less erosion. The DD is further classified into following classes

(1) Very low DD (Below 0-0.25 per 100km^2),

(2) Low DD (0.25-0.50 per 100km^2),

(3) Medium DD (0.50-0.75 per 100km^2),

(4) High DD (0.75-1.00 per 100km^2),

(5) Very high DD (above 1.00 per 100km^2)

Topographic Relative Relief (TRR)

The TRR is related to variations in height over a specified area covering one ridge and one valley. The computation of TRR is considered efficient due to its uniqueness for representation of a surface without considering the Absolute Sea Level (ASL). TRR is a function of height above the sea level, however there is a difference between local and altitudinal TRR. The TRR is further distributed in low, moderate, high and very TRRs as below in Figure 5,

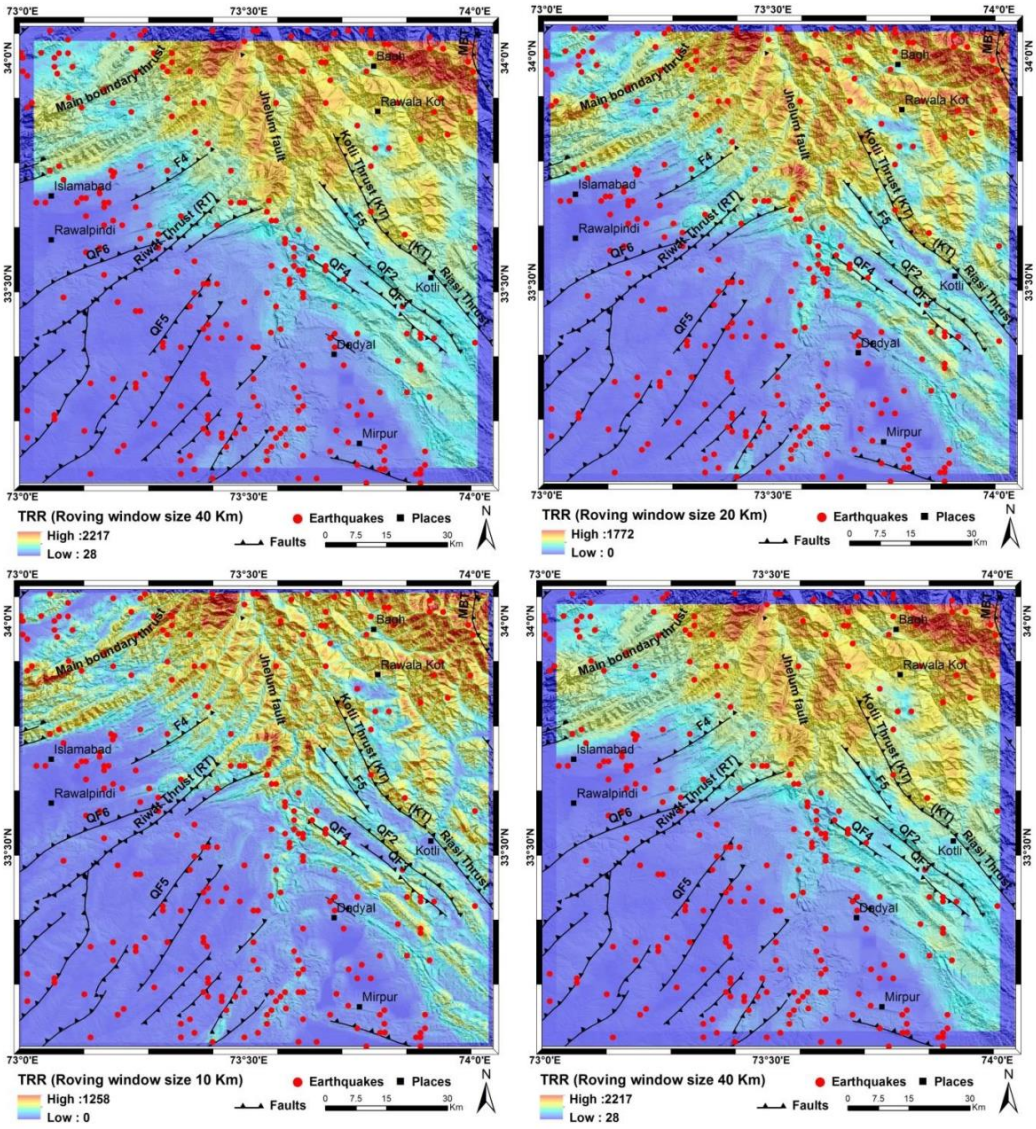

Figure 5. Topographic relative relief maps of investigation site with variable roving widow sizes.

Low TRR (Bluish Color)

The TRR map represents the inconsistency in the investigation site which cover only 20-25% of total area. In our case it engages lower valley slopes of study site.

Moderate TRR (Cyanic Color)

This kind of TRR covered about 25-30% area of study site. This area included ridges above and below the RT and KT, lower part of Jhelum, Riwat thrust and some areas of Main Boundary Thrust representing the gentle slopes of study site.

High TRR (Orange Color)

The category of TRR covered 30-35% in term of area of the study site. This group of TRR covered NW, eastern and northern side of investigation site which covered high uplift rates. The sites are around RT, KT, MBT and the Jhelum Fault.

Very TRR (Reddish Color)

This TRR covered 15-20% area of the study site. This type of TRR covered the upper reaches of Mangla catchment and the upper part of Hazara Kashmir Syntaxis (HKS). The footprints of this TRR were observed in the area of Bagh, Upper MBT, Upper Jehlum Fault, Bagh and Tawlakot as shown in Figure 5. This category of TRR falls in region of erosional/Tectonic scarps having very steepy slopes.

Topographic Vertical Dissection (TVD)

TVD describes, how a valley is dissected and advanced by erosional process in vertical direction. It was related to the slope variations in degrees, relative relief gradients as shown in Figure 6. The TVD map describes inhomogeneous spatially distributed bands of lower and higher values of TVD which relates to unraveling low and high dissection areas. Finally, the higher values of TVD are considered as recent uplift scenarios along KT, RT, MBT, Riwat Thrust and upper Jhelum Fault Figure 6. The higher values of TVD indicate the existence of lineaments in excess which represents that the topography is in youth and continuously uplifting due to neotectonics in the study site. Lower values of TVD were found in SE and SSE parts of intermountain watershed having fresh and active deposits and sedimentations. The high values of TVD were found in upper-central and Northern, NW and NE sides of study site which represent the existence of neotectonics in the study site.

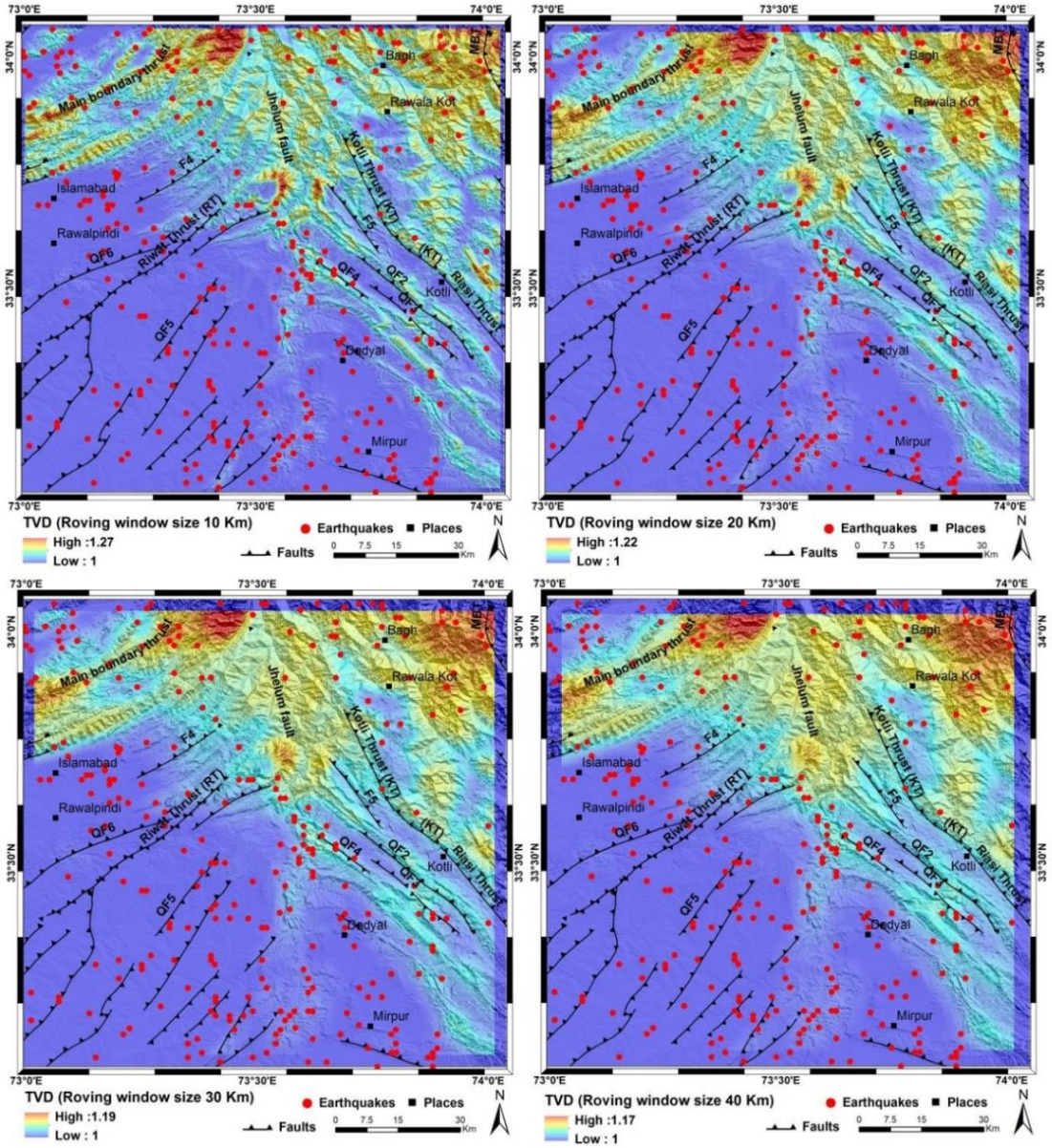

Figure 6. TVD maps for the study area with variable roving window size of 10, 20, 30 and 40Km.

Conclusions

The automated surface dynamic analysis performed using SRTM DEM which reveals that TRR characterizes spatially distributed topographic patterns and active structures within an investigation site. The TRR represents irregular disseminations, which relates to the existence of neotectonics in the study site. Lower values of TVD were in the SW of the study site. The highest values of TVD represent the instable landscape/topography present in N, NE, NW parts of study site. Various factors control drainage density e.g., climatic episodes, lithology, and topsoil permeability. The Iso Base Level map is efficient to demonstrate the active tectonic scraps and types of faults. Higher values of IBL were found in NE and in

Northern part of investigation site which indicates that the topography was younger or evolving. Finally, it is recommended that the outcomes can be used in evaluation of physical topographic examination, hydrology, tectonic geomorphology, environment, and ecology related management of study site.

REFERENCES

1. Golts, S. & E. Rosenthal, E. A morphotectonic map of the northern Arava in Israel derived form is obase lines. Geomorphology, 1993. 7: 305-315 (1993).
2. Grohmann, C.H., C. Riccomini, & F.M. Alves. SRTM-based morphotectonic analysis of the Po\\c cos de Caldas Alkaline Massif, southeastern Brazil, Computers & Geosciences. 33(1) :10-19 (2007).
3. Garrote,J., G.G.Heydt, & R.T.Cox. Multi-stream order analyses in basin asymmetry: A tool to discriminate the influence of neotectonics in fluvial landscape development (Madrid basin,central Spain). Geomorphology. 102 :130 -144 (2008).
4. Filosofov, V. Brief guide to morphometric methods in search of tectonic structures. Saratov: Saratov University Public House (1960). (Russian language).
5. Pennock, E., R.J. Lillie, A. Zaman, & M.Yousaf. Structural Interpretation of Seismic Reflection Data from the Eastern Salt Range and Potwar Plateau. Pakistan, Bull. Amer Assoc.Petrol. Geol.73(7) : 841-857(1989).
6. Lillie, R.J., G.D.Johnson, M. Yousaf, A.S.H. Zamin, & R.S. Yeats. Structural Development within the Himalayan Foreland Fold-And-Thrust Belt of Pakistan. Beaumont & Tankard (eds.) Sedimentary basins and basin forming mechanisms. Can Soc. Petro. Geol., Memoir. 73(7): 379-382 (1987).9
7. Mahmood, S. A. & R. Gloguen. Analysing spatial autocorrelation for hypsometric integral to discriminate neotectonics and lithologies using DEMs and GIS. GIScience and remote sensing.48(4): 541-565 (2011).
8. Strahler, A. N. Hypsometric (area-altitude) analysis of erosional topography, Geol. Soc. Am.Bull. 63(11): 1117 – 1142 (1952).
9. Grohmann, C.H., C. Riccomini, & M.A.C. Chamani. Regional scale analysis of landform configuration with base-level (isobase) maps. Hydrology and earth system sciences.15: 1493-1504 (2011).
10. Stewart, I. & P. Hannock. What is a fault scarp? Episodes,61: 256–263 (1990).
11. Zuchiewicz, W. & R. Oaks. Geomorphology and structure of the Bear River Range, north eastern Utah: a morphometric approach, Z. Geomorphol., Suppl.-Bd. 94: 41–55 (1993).
12. Sant'Anna, L. G., H.D Schorscher. & C. Riccomini. Cenozoic tectonics of the Fonseca Basin region, eastern Quadril´ateroFerr´ıfero, MG, Brazil, J. S. Am. Earth Sci. 10:275–284 (1997).
13. Mahmood, S. A., S. Siddiqui, V. Liesenberg, R. Gloguen, & M. Rahnama. DEM based analysis of active deformation in Hindukush using river profiles, surface dynamics and polynomial trend surfaces, (in review) Geomorphology, 2012.